Earthquake Engineering, Tenth World Conference © 1992 Balkema, Rotterdam. ISBN 90 5410 060 5

Foundation work for reduction of earthquake response

Kenji Miura, Yoshiharu Kiyota, Yasutsugu Suzuki & Masayuki Nagano
Kobori Research Complex Inc., Japan

Kikuo Ishimura
Tokyo Electric Power Company, Japan

ABSTRACT: This paper describes a foundation work for reducing the earthquake response of structures founded on firm rock. A high damping material is laid in the clearance between the basemat and the underlying rock, thus giving a higher damping factor to the structure and reducing its earthquake response. The effectiveness of this foundation work and the development of the high damping material are described.

1 INTRODUCTION

Nuclear power plant facilities in Japan have been and will continue to be founded on firm rock. As these facilities are rigid and massive, their dynamic behavior is strongly affected by dynamic soil-structure interaction(SSI). The damping factor attributable to SSI is almost proportional to non-dimensional frequency $a_0=\omega b/V_s$ (ω:circular frequency, b:width of foundation, V_s:shear wave velocity of underlying soil). As V_s increases with rock firmness, the earthquake response of a structure increases with the firmness of the rock on which it is founded. This paper describes a foundation work for reducing the earthquake response of a massive and rigid structure founded on firm rock.

Many devices have been proposed and adopted for reducing the earthquake response of structures. The base-isolation system, in which rubber bearing elements are installed between the base-slabs, is one such device (for example, Fujita(1991)). The basic concept of this system is to make the natural period of a structure longer than the period range in which the earthquake input motion is expected to be predominant. This base-isolation system may be effective against earthquakes in which the short period component is predominant, but can not be effective against earthquakes in which the long period component is predominant. Furthermore, it is expensive to install the base-isolation system in heavy structures such as nuclear power plant facilities, because of the large number of rubber bearing elements required to support their weight.

The foundation work described herein comprises laying a high damping material in the clearance between the basemat and the underlying rock, thus giving a higher damping factor to the structure and reducing its earthquake response. However, this foundation work is only useful for a massive and rigid structure founded on firm rock. This paper describes analytical examinations for checking the efficiency of the proposed foundation work and material tests for obtaining a suitable material for this foundation work.

2 BUILDING AND FOUNDATION WORK

A nuclear reactor building of the FBR (Fast Breeder Reactor) type was selected as the object of this research. It is assumed that it will be directly constructed on an outcrop of firm rock whose shear wave velocity V_s=2000m/sec., unit weight γ_t= 2.3t/m^3, and Poisson's ratio ν=0.4, and provides 1% hysteresis type damping. The building will be 63m high from the bottom to the roof and it will weigh 200,000tons. The basemat will be 63mx65.5m and 5m thick.

According to the usual construction method (UCM), the basement would be buried in the rock with a 3m side clearance between the side wall and the rock. After completing the basemat construction, this side clearance would be filled with concrete. However, in the proposed foundation work for reduction of earthquake response (FWRE), the rock underneath the basemat will be excavated by D meters, and this excavation will be paved with a high damping material (HDM). The side clearance will be also filled with HDM. Fig.1 illustrates the FWRE.

3 ANALYTICAL EXAMINATION

3.1 *Analytical conditions*

An analytical examination was performed to check the effectiveness of the FWRE. The FEM model shown in Fig.2 was employed in this examination. The boundary conditions of this model are an energy transmitting boundary on the side and viscous damping on the bottom. The basemat was treated as a rigid disc with an area equal to that of the basemat. The building was modeled by a stick comprising 11 lumped masses. These masses are connected by columns with assumed shearing and flexural rigidities. 5% hysteresis type damping is given to the building model. To inspect the accuracy of the FEM model, the dynamic impedance functions for a rigid surface foundation on homogeneous rock derived by the analytical and FEM methods were compared as shown in Fig.3. The FEM

model conformed well to the analytical solution based on 3-dimensional wave propagation theory, and is applied in the examination hereafter.

The physical constants of the HDM were assumed to be V_s=400m/sec., ν=0.3 and γ_t=2.2t/m^3. The thickness D and the damping factor h_m of the HDM were selected as analytical parameters.

3.2 *Dynamic impedances*

The dynamic impedance of the foundation is expressed by a function whose real part indicates the rigidity of the underlying media and the imaginary part the damping. As the HDM is softer than the rock, the real part decreases with the FWRE. The imaginary part is caused by geometrical damping (radiation damping) and the material damping of the media surrounding the foundation. Since part of the radiation wave from the foundation into the underlying HDM is reflected at the interface between the HDM and the underlying rock and returns to the foundation, the radiation damping is decreased by the FWRE. However, the material damping is increased by the HDM. Fig.4 shows the dynamic impedances with changing D of the HDM. The damping factors h_d of the dynamic impedances evaluated by Eq.(1) are drawn in Fig.5.

$$h_d = sin\{0.5tan^{-1}(K_I/K_R)\} \qquad (1)$$

where; K_R and K_I are the real and the imaginary parts of the dynamic impedances.

Both the real and the imaginary parts decrease rapidly with slightly increasing D when D is relatively thin, while both reach stability for D=4m or 5m. The h_d of the FWRE becomes larger than UCM in the lower frequency range, but smaller in the higher frequency range. The critical frequency f_c is recognized as that at which the h_d of the FWRE is equal to that of the UCM. The FWRE is understood to be effective for a building whose natural frequency is lower than f_c. f_c for rocking impedance is higher than that for swaying. This is because the radiation damping of rocking impedance itself is smaller than that of swaying impedance and the effect of the HDM on providing higher damping is more remarkable in rocking impedance.

3.3 *Natural frequency and vibration mode*

Fig.6 shows the relation between the natural frequencies and D of the HDM. With D=5m, the first and the second natural frequencies come to about 85% of those of the UCM. Fig.7 depicts the vibration modes for D=5m. The FWRE brings about larger lateral translation at the basemat and smaller participation factors β.

3.4 *Response characteristics*

The response characteristics are inspected when the shear wave propagating upward attacks the building on the FWRE. The frequency transfer functions of the lateral translation of the building to that at the surface of the free field rock are shown in Fig.8 for changing D of the HDM. The resonance frequencies become lower and the magnification factors for the upper positions of the building at the resonance peak become smaller with increasing D. However, the magnification factor for the lower position such as the basemat increases. This specificity is because the FWRE reduces the rocking component and increases the lateral translation of the basemat. Fig.9 shows the magnification factors for D=5m with increasing damping factor h_m of the HDM. To obtain a significant FWRE, the HDM must provide a damping factor of over 15%. Fig.10 shows the magnification factors of overturning moment at the basemat. The FWRE reduces the overturning moment and the bothersome foundation uplift problem.

4 HIGH DAMPING MATERIAL

4.1 *Selection of material*

According to the above analytical examinations, to obtain a significant FWRE, the HDM must provide a damping factor of over 15%. There are many kinds of materials which have high damping capacity. However, since the HDM is lain underneath the basemat in the proposed FWRE and its volume is huge, it must be inexpensive. The ordinary average vertical pressure σ_v in the HDM amounts to around 5.0 kg/cm^2 and the HDM must withstand the large vertical pressure. Moreover, it must be of excellent durability and workability. Based on these requirements, the authors selected a mixture of gravel and asphalt termed Asphalt Gravel(AG). The gravel can be obtained easily at the construction site after the excavation of the rock and the excellent workability of AG has been proved by the past road pavement works. The element tests described below were carried out to obtain the dynamic and static properties of AG.

4.2 *Material and test procedure*

Two kinds of aggregates were made by mixing gravel with sand and mineral filler. Table 1 indicates the properties of the aggregates and Table 2 the properties of the asphalt. After warming the asphalt until it became fluid, it was poured onto the aggregates to produce the asphalt gravel(AG). The test specimens were produced by putting this AG in a mold and compacting it with a vibrator. The asphalt content was decided so as to obtain the most suitable content ratio determined by the Marshal stability test for asphalt pavement work. The large dynamic simple shear test apparatus shown in Fig.11 was used for the dynamic shear deformation tests and the triaxial compression apparatus was employed for the strength tests. The test specimens were 300mm in diameter and 100mm in height for the deformation tests, and 100mm in diameter and 200mm in height for the strength tests.

The tests were performed at a room temperature of 22 degrees. The test conditions of the deformation tests are tabulated in Table 3. The first characters I and II of the test No. in this table denote specimens made from the aggregates I and II shown in Table 1, the second G and AG indicate the aggregate only and the asphalt gravel, and the last character shows the kind of test.

The AG must be mainly durable against water. Permeability tests were performed, but no water permeated through the AG specimens. The AG in the

FWRE will be lain underneath the basemat and never exposed to ultraviolet rays. Thus, it can be judged to be sufficiently durable.

4.3 *Test results*

(1) *Dynamic shear modulus and damping factor*
The dynamic shear deformation tests were performed under a vertical stress σ_v=3.0kg/cm^2. The relations between shear modulus G, damping factor h_m and shear strain γ for the aggregates(G) and AG are shown in Fig. 12 and Fig.13. G_o denotes the initial shear modulus, which means that at the very low shear strain γ=0.0001%. Thus, the vertical axis G/G_o indicates the decreasing ratio of rigidity. No difference occurs due to the different kinds of aggregates I and II. No distinct variation of G/G_o-γ relations is recognized between the aggregates and AG. The damping factor h_m is very small for the aggregates, while AG has a very high damping capacity. In particular, AG has 15% damping factor even at low strain levels. When the design earthquake attacks the building on the FWRE, the effective shear strain in the HDM is estimated to be around 0.02% and h_m of AG at this strain level amounts to about 20%. It can be said that the rigidity-strain relation of the aggregates is maintained and damping only is added to the aggregates. Hysteresis loops are drawn in Fig.14. The loop of AG exhibits a rounder and more obvious slip type loop than that of the aggregates.
(2) *Dependence on vertical stress*
Dependence of the initial shear modulus G_o and damping factor h_m on the vertical stress σ_v are shown in Fig.15 and Fig.16. G_o of AG is larger and its dependence on σ_v is weaker than that of the aggregates. h_m of AG decreases slightly with increasing σ_v.
(3) *Dependence on frequency*
By changing the excitation frequency in steps under σ_v=3.0kg/cm^2, the dependence on frequency was examined as shown in Fig.17 and Fig.18. Little frequency dependence is observed for the aggregates, while AG exhibits considerable dependence. G_o of AG becomes larger and h_m also slightly larger with increasing frequency. Because G_o of AG approaches that of the aggregates at lower frequencies such as 0.01Hz, it can be judged that the static properties of AG are similar to those of the aggregates.

(4) *Strength*
The test conditions and results for the static triaxial compression tests are shown in Table 4 and Fig.19. Since the internal friction angle ϕ of AG is smaller but the cohesion C of AG is larger than those of the aggregates, the strength of AG becomes larger under confining stresses lower than 7.0 kg/cm^2. Furthermore, AG exhibits more ductile properties after a large strain has been applied.
(5) *Summary of material tests*
According to the test results described above, the shear modulus of AG is found to be equal to or lager than that of the aggregates. The strength of AG becomes larger than that of the aggregates and the damping factor h_m amounts to more than 15% only under the low strain level. The damping factor amounts to 20% at the strain level due to the design basis earthquake for nuclear power plant facilities in Japan.

5 CONCLUSIONS

A foundation work was proposed for reduction of earthquake responses of buildings on firm rock. This foundation work comprises paving a high damping material underneath the basemat of the building. The analytical examination demonstrates the efficiency of this foundation work if the high damping material has a damping factor above 15%. A mixture of gravel with asphalt was selected as being the most suitable for this foundation work. Element tests showed that this material exhibits the properties required for the proposed foundation work.

REFERENCE

Fujita, T. 1991, Seismic isolation and response control for nuclear and non-nuclear structures, Special Issue for the Exhibition of the 11-th International Conference on Structural Mechanics in Reactor Technology

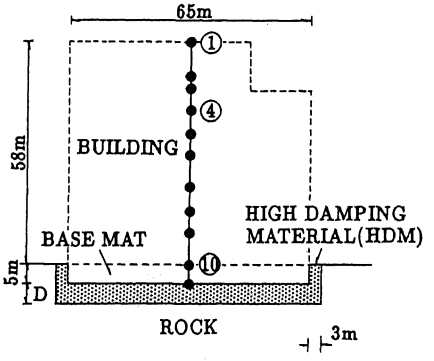

Fig.1 Proposed foundation work (FWRE)

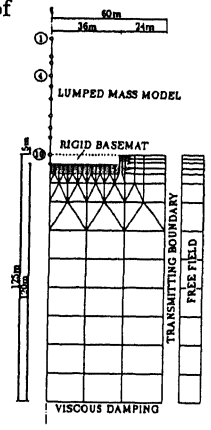

Fig.2 FEM model

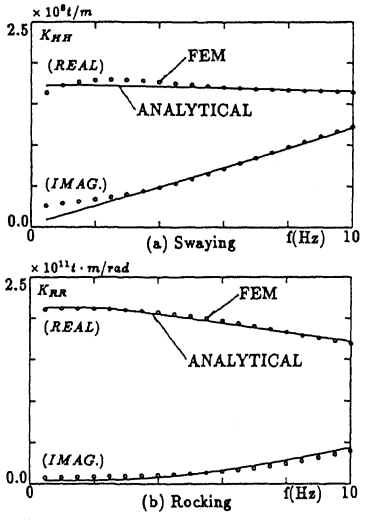

Fig.3 Comparison of dynamic impedances

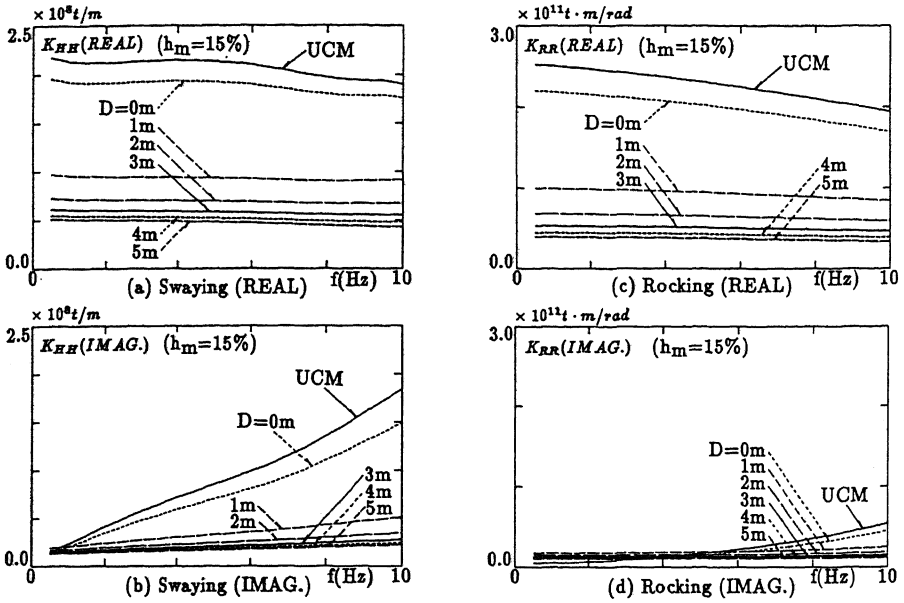

Fig.4 Dynamic impedances of foundation on FWRE

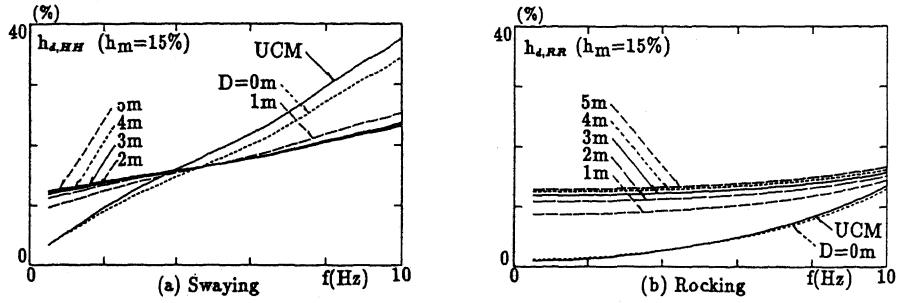

Fig.5 Damping factors h_d of dynamic impedances

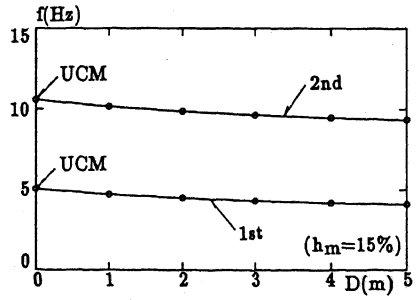

Fig.6 Natural frequencies vs. D of HDM

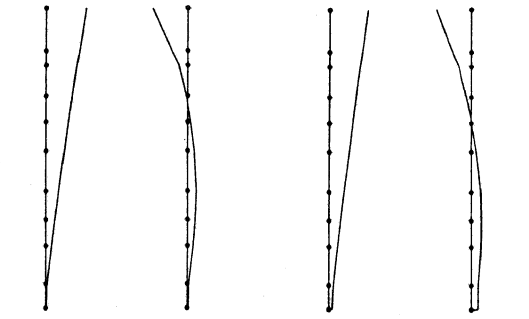

Fig.7 Natural frequencies and vibration modes

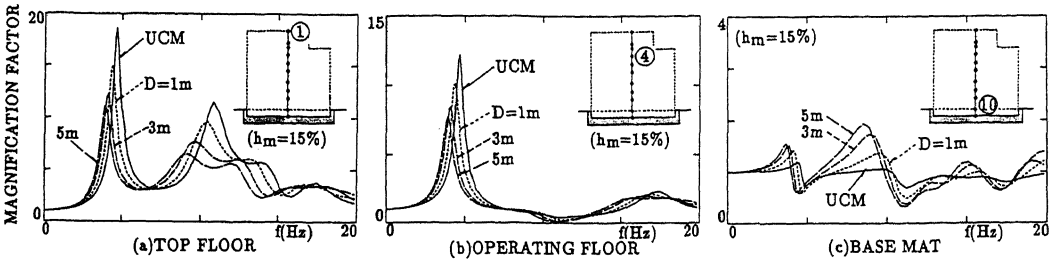

Fig.8 Transfer functions of lateral translation with increasing D

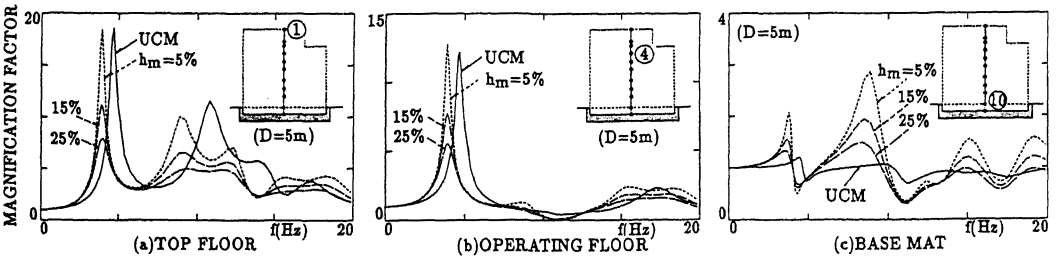

Fig.9 Transfer functions of lateral translation with increasing h_m

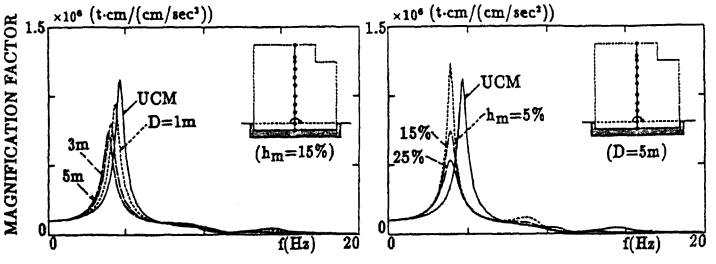

Fig.10 Transfer functions of overturning moment at basemat

Table 1 Physical properties of aggregates

Aggregate	Gs	D_{50} (mm)	Uc
No. I	2.730	3.2	26.0
No. II	2.723	0.59	18.0

Gs : Specific gravity of soil particle
D_{50}: Mean grain size
Uc : Uniformity coefficient

Table 2 Physical properties of asphalt

Items	Value
Asphalt type	Straight asphalt
Penetration at 25 ℃	69
Softening point (℃)	47.5
Specific gravity	1.026

Table 3 Test conditions of dynamic deformation tests

Test No.	Test type	Ac (%)	γ_t (gf/cm³)	Gs'	e	f (Hz)	σ_v (kgf/cm²)
I–G –γ	γ test	0.0	2.193	2.730	0.245	1.0	3.0
II–G –γ	γ test	0.0	2.108	2.723	0.292	1.0	3.0
I–AG–γ	γ test	5.6	2.366	2.498	0.056	1.0	3.0
II–AG–γ	γ test	9.0	2.246	2.370	0.055	1.0	3.0
I–G –σ	σ test	0.0	2.257	2.730	0.210	1.0	0.7~5.0
II–G –σ	σ test	0.0	2.097	2.723	0.299	1.0	0.7~5.0
I–AG–σ	σ test	5.6	2.358	2.498	0.059	1.0	0.7~5.0
II–AG–σ	σ test	9.0	2.223	2.370	0.066	1.0	0.7~5.0
I–G –f	f test	0.0	2.257	2.730	0.210	0.01~5	3.0
II–G –f	f test	0.0	2.097	2.723	0.299	0.01~5	3.0
I–AG–f	f test	5.6	2.358	2.498	0.059	0.01~5	3.0
II–AG–f	f test	9.0	2.223	2.370	0.066	0.01~5	3.0

γ test: Dynamic deformation test for various shear strains, γ
σ test: Dynamic deformation test for various vertical stresses, σ_v
f test: Dynamic deformation test for various frequencies, f
Ac : Asphalt content γ_t : Unit weight
Gs': Equivalent specific gravity of soil particle considering asphalt content
e : Void ratio σ_v : Vertical stress f : Frequency

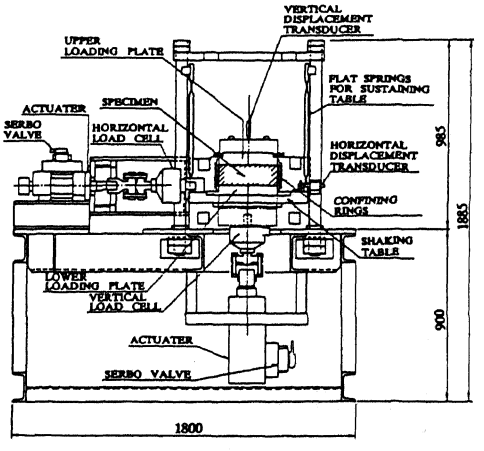

Fig.11 Large dynamic simple shear test apparatus

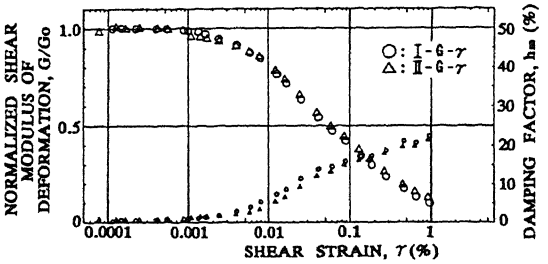

Fig.12 Shear modulus and damping vs. shear strain for aggregates

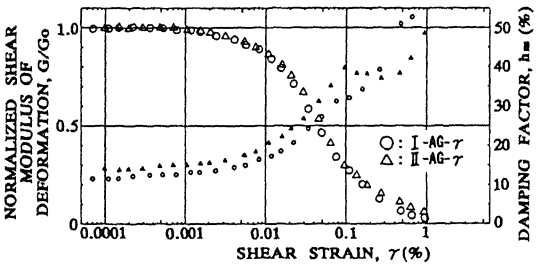

Fig.13 Shear modulus and damping vs. shear strain for AG

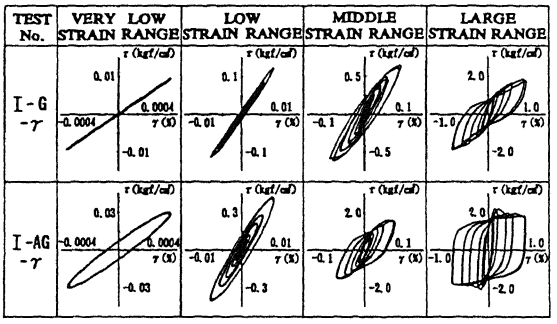

Fig.14 Hysteresis loops

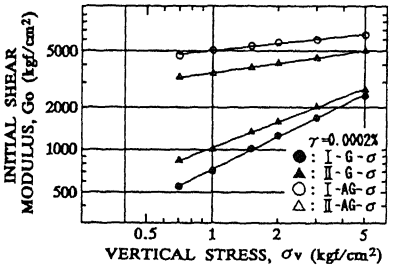

Fig.15 Initial shear modulus vs. vertical stress

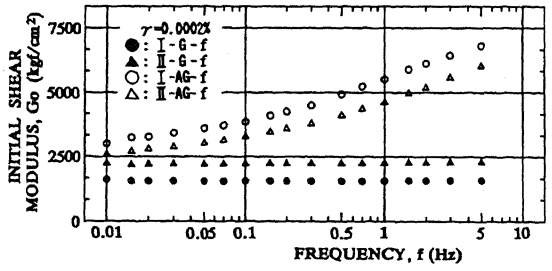

Fig.17 Initial shear modulus vs. frequency

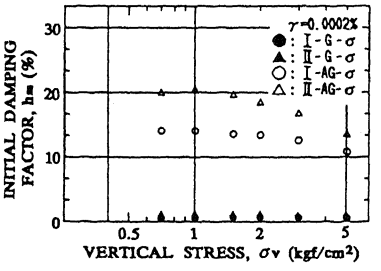

Fig.16 Initial damping factor vs. vertical stress

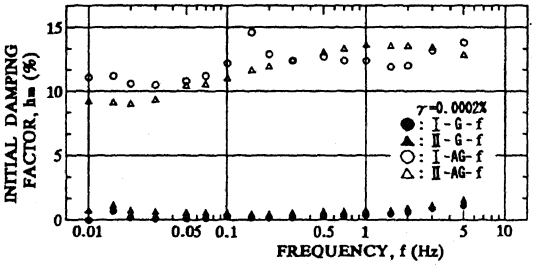

Fig.18 Initial damping factor vs. frequency

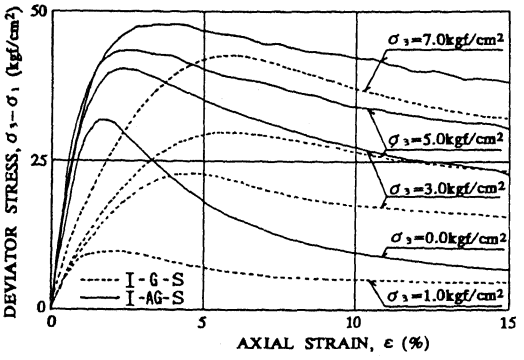

Fig.19 Deviator stress vs. axial strain

Table 4 Strength test results

Test No.	Test type	σ_c (kgf/cm²)	C (kgf/cm²)	ϕ (deg.)	ε_f (%)
I–G –S	S test	1.0~7.0	0.95	46.6	2.0~6.0
II–G –S	S test	1.0~7.0	0.53	47.0	2.5~6.5
I–AG–S	S test	0.0~7.0	8.76	32.4	2.0~4.0
II–AG–S	S test	0.0~7.0	6.48	33.5	4.5~8.0

S test: Strength test
σ_c : Confining stress
C : Cohesion
ϕ : Internal friction angle
ε_f : Peak strain